Comparison of quantum mechanical and empirical potential energy surfaces and computed rate coefficients for N_2 dissociation

Richard L. Jaffe[1] and David. W. Schwenke[2],
NASA Ames research Center, Moffett Field, CA 94035-1000
Maninder Grover[3], Paolo Valentini[4] and Thomas E. Schwartzentruber[5]
University of Minnesota, Minneapolis, MN 55455
and
Simone Venturi[6] and Marco Panesi[7],
University of Illinois at Urbana-Champaign, Urbana, IL 61801

Comparisons are made between potential energy surfaces (PES) for N_2 + N and N_2 + N_2 collisions and between rate coefficients for N_2 dissociation that were computed using the quasiclassical trajectory method (QCT) on these PESs. For N_2 + N we compare the Laganà's empirical LEPS surface with one from NASA Ames Research Center based on *ab initio* quantum chemistry calculations. For N_2 + N_2 we compare two *ab initio* PESs (from NASA Ames and from the University of Minnesota). These use different methods for computing the ground state electronic energy for N_4, but give similar results. Thermal N_2 dissociation rate coefficients, for the 10,000K-30,000K temperature range, have been computed using each PES and the results are in excellent agreement. Quasi-stationary state (QSS) rate coefficients using both PESs have been computed at these temperatures using the Direct Molecular Simulation of Schwartzentruber and coworkers. The QSS rate coefficients are up to a factor of 5 lower than the thermal ones and the thermal and QSS values bracket the results of shock-tube experiments. We conclude that the combination of *ab initio* quantum chemistry PESs and QCT calculations provides an attractive approach for the determination of accurate high-temperature rate coefficients for use in aerothermodynamics modeling.

Introduction

Physics-based modeling of hypersonic flows is predicated on the availability of chemical reaction rate coefficients and cross sections for the collisional processes. This

[1] Senior Research Scientist, NASA Ames Research Center Aerothermodynamics Branch, Mail Stop 230-3, Moffett Field, CA 94035-1000, Associate Fellow AIAA. richard.jaffe@nasa.gov
[2] Senior Research Scientist, NASA Ames Research Center, NAS Applications Branch, Mail Stop 258-3, Moffett Field, CA 94035-1000.
[3] Graduate Student, Department of Aerospace Engineering and Mechanics, University of Minnesota, Minneapolis, MN 55455, Student Member AIAA
[4] Post Doctoral Fellow, Department of Aerospace Engineering and Mechanics, University of Minnesota, Minneapolis, MN 55455, Member AIAA
[5] Associate Professor, Department of Aerospace Engineering and Mechanics, University of Minnesota, Minneapolis, MN 55455, Senior Member AIAA
[6] Graduate Student, Department of Aerospace Engineering, University of Illinois at Urbana-Champaign, 104 Wright St., Urbana, IL 61801.
[7] Assistant Professor, Department of Aerospace Engineering, University of Illinois at Urbana-Champaign, 306 Talbot Lab, 104 Wright St., Urbana, IL 61801, Senior Member AIAA

approach has been built around the use of quantum mechanical calculations to describe the interaction between the colliding particles and is described in detail in Ref. 11. In this approach, a potential energy surface (PES) is computed by solving the electronic Schrödinger equation and collision cross sections are determined for that PES using classical, semiclassical or quantum mechanical scattering methods. Reaction rate coefficients are computed by integrating the cross sections with the appropriate Maxwell-Boltzmann weighting. State-to-state rate coefficients are determined by integrating over a Maxwellian distribution of collision energies. Finally, thermal rate coefficients are determined by summation of the Boltzmann-weighted state-to-state rate coefficients for reactions of molecules in all relevant ro-vibrational energy levels. If the flow is in thermal non-equilibrium, the translational, vibrational and rotational energy modes can be represented in different ways: (1) the rovibrational energy modes can be described by an internal temperature that is distinct from the translational temperature T, (2) three different temperatures (for translation, vibration and rotation) can be used to describe the distributions, or (3) the populations of individual ro-vibrational energy levels can be determined by solving the Master Equation[2], or through the use of Direct Molecular Simulation[3]. The PES-to-rate coefficient approach had been proposed and attempted in the early days of digital computing, but it is only in the last 15 years that computer hardware and software have been up to the task of calculating accurate interatomic and intermolecular potentials and determining state-to-state reaction cross sections or rate coefficients.

Recently several new "first principles" potential energy surfaces to describe ro-vibrational energy transfer and dissociation in molecular nitrogen have become available. These have been computed by solving the quantum mechanical Schrödinger equation for the electronic energy of three or four nitrogen atoms at a large number of geometric arrangements. The resulting energies are fit to an analytical expression for rapid interpolation of the energy for any arbitrary geometry and have been used in quasiclassical trajectory (QCT) calculations to determine collision cross sections and reaction rate coefficients for inelastic and dissociative processes. Examples for N_2 + N collisions are the PESs from NASA Ames Research Center[4-5], the L4 PES from the Universidad del Pais Vasco, Spain[6] and a PES from the Universidade de Coimbra in Portugal[7]. For N_2 + N_2 collisions there are PESs from NASA Ames[8], the University of Minnesota[9] and the Università di Perugia[10].

Possibly the earliest example of a PES dates to 1931 with the empirical potential of *Eyring* and *Polanyi*[11] for the interaction of three hydrogen atoms, which was based on the theoretical Valence Bond theory treatment of *London*[12] for H_3. This was later made more general by *Sato*'s[13,14] addition of an overlap parameter and used for QCT of atom-diatom exchange reactions involving hydrogen and halogen atoms (hence the acronym *LEPS*). This empirical potential has a simple analytical form and has been widely used for computations of simple collisional processes involving three or four atoms (e.g., atom + diatom and diatom + diatom collisions). The H_3 LEPS potential was used by Erying and others for Transition State Theory[15] calculations of rate coefficients and by Karplus et al. for QCT calculations of atom-diatom collisions[16]. Laganà et al.[17] generated a LEPS potential for N_2 + N collisions that has been used by Esposito and coworkers[18] for QCT calculations of state-to-state N_2 energy transfer

and thermal homogeneous exchange and dissociation rate coefficients. For an atom-diatom system (designated A + BC), a PES generated using the LEPS formalism exhibits a preference for a collinear arrangement of the three atoms, with an energy barrier that can be adjusted by varying the Sato parameter. The minimum energy path for the exchange reaction A + BC → AB + C traverses this barrier. For N_2 + N, the LEPS surface has an energy barrier of 36 kcal/mol. In contrast, the ab initio PESs [4-7] have energy barriers of 44-47 kcal/mol for the exchange pathway with a bent transition state (the N-N-N angle is 116-118^o). Furthermore, this transition state has unequal N-N bond lengths and there is a shallow energy well at the symmetric geometry.

In order to use a quantum mechanical PES for simulating collisional processes it must be represented by an analytical function. The PES is computed for a geometric grid and the set of geometries and energies must be accurately represented by that multi-parameter function. The process of determining the functional form and values for the parameters that reproduce these energies is quite tedious and time consuming, because it involves non-linear fitting in many dimensions. Three and four atom systems have three and six geometric variables, respectively. Each research group has their own recipe for devising the geometric grid, computing the electronic energy (i.e., the atomic orbital basis set expansion and treatment of electron correlation effects used in solving the electronic Schrödinger equation) and defining the analytic expression used to represent the PES. As a result, when there are two or more PESs for a given collisional system, it is likely that there will be differences between the potentials and between QCT rate coefficients computed using each PES.

With all these potentials available for use, the obvious questions arise, such as: ***how do these PESs compare, how sensitive are QCT cross sections and rate coefficients to the accuracy of the PES, and, most importantly, what cross sections or rate coefficients should be used for Direct Simulation Monte Carlo (DSMC) and Computational Fluid Dynamics (CFD) flow field calculations***? In this paper, comparisons will be made between the different PESs and between thermal and phenomenological rate coefficients computed using them. The most complete datasets of cross sections and rate coefficients have been obtained using the NASA Ames[8] and University of Minnesota[9] PESs for N_2 + N and N_2 + N_2, so those comparisons will be the major emphasis of this paper. The rate coefficient comparisons will be made for collisional dissociation under thermal equilibrium[2,19-20] and quasi-steady state (QSS) conditions[2,3]. Work at Ames[2] and Minnesota[3] have used 0-d Master Equation (ME) and Direct Molecular Simulation (DMS) methods to compute phenomenological (i.e., QSS) dissociation rate coefficients, which take into account energy transfer and other collisional processes such as exchange and recombination reactions. For this study, we will compare dissociation rate coefficients for N_2 + N and N_2 + N_2 computed with these potential energy surface. For N_2 + N we compare the LEPS and NASA and for N_2 + N_2 we compare the NASA and Minnesota potentials, as these have been used for QCT calculations of dissociation rate coefficients. As both the NASA Ames and U. Minnesota potentials for N_2 + N_2 are independently constructed and free from empirical calibration, the results of these comparisons should provide validation of this aspect of the physics-based approach to hypersonic chemistry models.

Description of the "NASA" and "Minnesota" Potentials for $N_2 + N_2$

The potential energy surfaces generated to describe $N_2 + N_2$ collisions at NASA Ames Research Center and the University of Minnesota (hereafter called the NASA PES and Minnesota PES, respectively) are based on similar quantum chemistry methods [1,8,9]. In these calculations, the electronic Schrödinger equation is solved, approximately, by a double expansion technique. This is carried out for a fixed geometric arrangement of the nuclei. First a basis set expansion of atomic orbital functions is used and the Schrödinger equation is solved in the approximation that each electron feels the average Coulombic forces of all the other electrons (called the Hartree-Fock solution, or HF). This step results in the generation of a set of molecular orbitals that are linear combinations of the atomic orbital basis. Then the HF approximation is removed in a sequence of steps that account for the true electron-electron interactions (called electron correlation). This part of the calculation uses a basis of electron configurations, i.e., different arrangements of the electrons in the molecular orbitals. The calculated electronic energy approaches the exact solution of the Schrödinger equation as the two basis expansions become infinite. These calculations are repeated for each geometric arrangement of the atoms to generate a set of geometries and energies to describe the interactions between the atoms. For the N_4 system, the goal of these calculations is to accurately represent the energy of the atoms relative to some reference geometry (e.g., two N_2 molecules at their equilibrium bond lengths, r_e, and separated by a very large distance). An accuracy of ±5 kJ/mol is often considered "chemical accuracy", meaning the potential can be used for computing reaction rate coefficients with accuracies comparable to modern experimental methods.

The NASA and Minnesota PESs are based on the same atomic orbital basis, the so-called augmented correlation-consistent polarized valence triple zeta basis[21,22]. The NASA PES utilized two different methods to compute the electron correlation. The coupled cluster method (CCSD(T))[23] was used for geometries where there are two distinct N_2 molecules and the multi-reference configuration interaction method (MRCI)[24] was used for other geometries. The latter method used complete active space (CASSCF)[25] molecular orbitals instead of Hartree Fock. This approach includes the most important electron correlation effects in the orbital optimization process, and also speeds up the convergence of the MRCI expansion. The CCSD(T) method requires considerably less computer time per geometry than does the CASSCF-MRCI method. For the N_4 PES, the CCSD(T) method was used for 3821 geometries and the CASSCF-MRCI method was used for 325 geometries. For the CCSD(T) calculations, the 2s and 2p electrons were included in the calculation (5 eletrons per N atom, thus the 1s electrons were kept in the Hartree-Fock orbitals), while for the CASSCF-MRCI calculations only the 2p electrons (3 electrons per N atom) were included for the CASSCF and all the 2s and 2p electrons were included for the MRCI. Several classes of geometries were used: linear, planar (rectangular, trapezoidal and T-shaped) and various non-planar arrangements. For all of these sets of geometries, both N_2 bond lengths were varied from the r_e – 0.2 Å to 5 Å.

For the NASA PES, these N_4 energies were fit to a complicated function that describes the potential energy in terms of six geometric variables. This fitting function

uses a 2-body term $V^{(2)}$ (the N_2 diatomic potential calculated by the same MRCI method as used for N_4) summed up for each of the six N-N pairs that are possible and an interaction term $V^{(INT)}$ which is fit to $\{E_i - \Sigma_j V^{(2)}_j\}$ where the E_i represent the calculated potential energies for the set of geometries. Owing to the fact that different quantum mechanical methods were used, CCSD(T) and MRCI energies for the same geometry are not the same. So all of the CCSD(T) energies were scaled by a single multiplicative factor that was determined in the fitting process of fitting $V^{(INT)}$. An additional expression is used to ensure the fitted potential exhibits the correct long-range behavior when the two N_2 molecules or a triatomic molecule and atom are separated by more than 5 Å. This behavior is also built into the 2-body term. Finally, after the fitting parameters have been optimized to fit the quantum mechanical energies, the 2-body term for N_2 is replaced by an accurate empirical expression. This ensures that the PES reproduces the correct ro-vibrational levels and long-range form for N_2. We use the potential derived by LeRoy[26] modified to have more accurate behavior in the repulsive region (when $r < r_e - 0.2$ Å). For this PES, an N_2 molecule has 9390 ro-vibrational levels with 61 vibrational levels for J=0. The maximum rotational quantum number is 279 (for v=0). Of these (v,J) levels, 1969 are quasibound, meaning they lie above the dissociation limit, but lower than the centrifugal barrier for a particular value of J. The quasibound levels can spontaneously dissociate by tunneling, but most of them have lifetimes that are long compared to the time between collisions. The determination of the ro-vibrational energy levels was carried out using the semiclassical WKB method[27], which closely approximates the fully quantum mechanical results. A more detailed discussion of the quantum mechanical calculations and PES fitting process can be found in Ref. 1.

The Minnesota PES[9] is based on quantum mechanical calculations that are similar to those described above. The same atomic orbital basis set is used (except that some of the d- and f-orbitals are dropped from the augmentation set). A similar CASSCF procedure is used to obtain the molecular orbitals, but second-order perturbation theory was used in place of MRCI. That method is called CASPT2 [28]. Only the 2p electrons are included in the CASPT2 calculations. The use of the smaller augmentation and exclusion of the 2s electrons results in an N_2 dissociation energy of 228.7 kcal/mol that is in excellent agreement with the experimentally determined value of 228.4 kcal/mol. In contrast, a calculation with the same atomic orbital basis set, but with all the 2s and 2p electrons included, yielded a dissociation energy of 220.3 kcal/mol. The Minnesota N_2 potential has 55 vibrational levels (6 fewer than the NASA N_2 potential) and the maximum value for J is 279 (same as for the NASA PES). In all there are 9198 ro-vibrational levels for N_2 with this potential, 7122 levels are bound and 2076 are quasibound. The calculation of the ro-vibrational energy levels was carried out using the same WKB method described above. The difference in the number of ro-vibrational levels reflects a difference in the long-range behavior of the two potentials. This can be seen in Figure 1. These calculations were carried out for 15363 geometries describing $N_2 + N_2$ and 1017 additional geometries describing $N_3 + N$. As a result, the resulting PES was expected to represent both $N_2 + N_2$ and $N_2 + N$ collisions. These geometries included nine sets of $N_2 + N_2$ arrangements and 3 sets of $N_2 + N$ arrangements. Within each set of $N_2 + N_2$ geometries, one N_2 bond length was varied between 0.8 and 6.0 Å and the other has fixed at re and $r_e \pm 0.2$ Å. Therefore, these geometries describe situations where only one of the molecules is highly vibrationally

excited or dissociating. The distance between centers of mass of the N_2 molecules was varied between 1 and 10 Å. The fitting function for the Minnesota PES is similar to that described above. The 2-body potential is the CASPT2 N_2 potential energy curve and the $V^{(INT)}$ was fit to the quantum mechanical energies minus the sum of 2-body energies. The process was simpler than in the NASA case, because there was only one computational method used.

As an example, the comparison between the NASA and Minnesota PESs for rectangular N_4 geometries is shown in Figure 2. In this arrangement, two N_2 molecules (both with bond length r) are a distance R apart. R (in bohr) is plotted along the x-axis and r (in bohr) is plotted along the y-axis. Each contour line represents a constant value of the N_4 potential energy relative to the energy of two N_2 molecules at $r = r_e$ and $R = \infty$. The red line represents zero energy and each successive blue line represents an increase in energy of 5 kcal/mol. The green line on the bottom plot is the locus of points with r = R (square geometries). One can see that for the two cases (NASA and Minnesota) the PESs are quite similar. For the low energy region around the $r \cong r_e$ and $R \geq 5$ bohr, the channel in the NASA PES is narrower in r and shallower in R. Other small differences can be seen throughout the contour plots.

Quasiclassical Trajectory Calculations of N_2 Dissociation Rate Coefficients

Given a potential energy surface that represents a pair of colliding atomic or molecular species, collision cross sections and rate coefficients can be simulated using classical mechanics using Hamilton's equations.[1] These describe the time evolution of positions and momenta of all the atoms involved in the collision. The interatomic forces are given by the derivative of the potential energy with respect to the position coordinates. One starts a collision with the species well separated and numerically integrates the trajectory as the atoms or molecules approach, interact and separate. Initially any molecules involved in the collision have rotation and vibration that corresponds to quantized levels. Their orientation and vibrational phase and impact parameter are randomly assigned, and the relative collision energy (E_{rel}) is specified. After the collision the products may be different from the initial state of the reactants due to ro-vibrational energy transfer (inelastic processes) or reaction (exchange or dissociation). The rotational and vibrational levels of the products are no longer quantized, due to the use of classical mechanics, but quantum numbers maybe assigned by binning. Usually thousands or millions of trajectories are computed and the overall reaction or energy transfer probabilities are used to compute collision cross sections. If the collision energy is fixed, the collision cross section is given by $S_r(E_{rel}) = \pi \times b_{max}^2 \times P_r$, where P_r is $N(i)/N_{tot}$ the probability of a specific outcome (e.g., dissociation of an N_2 molecule) – that is the number of occurrences (N(i)) in a batch of N_{tot} trajectories. If E_{rel} is sampled from a thermal distribution (at temperature T), the probability is proportional to a thermal state-to-state rate coefficient at that temperature. The rotation and vibration energies can also be sampled from thermal distributions at the same or different temperatures. Due to the Monte Carlo methodology used for the random sampling, the statistical error is roughly proportional to $N_{tot}^{-1/2}$. For $N_2 + N$ using the NASA Ames N_3 PES, state-to-state rate coefficients for energy transfer, exchange and dissociation were

computed for N_2 in each of the 9390 ro-vibrational levels.[1,2] For $N_2 + N_2$, thermal dissociation rate coefficients have been computed using both the NASA[29] and Minnesota[19,20] PESs. The NASA Ames state-to-state rate coefficients for N_2+N have been used in (ME) simulations of N_2 dissociation and thermal relaxation in the presence of a small amount of atomic nitrogen [2], yielding dissociation rate that correspond to QSS conditions. In this calculation, internal temperature is not used. Instead, the population of each ro-vibrational level is tracked as the relaxation progresses toward thermochemical equilibrium.

Direct Molecular Simulation Method

The DMS method is essentially the direct simulation Monte Carlo (DSMC) method [30] where all stochastic collision models are replaced by trajectory calculations performed on a potential energy surface (PES). It was first developed by Koura who called it the classical trajectory calculation DSMC.[31-33] The Direct Molecular Simulation (DMS) method and the QCT method involve integration of many trajectories between pairs of particles. The major difference between the two methods is that in a QCT calculation, initial collision pairs are sampled from a Boltzmann distribution and the pre- and post collision states of the particles are used to determine bulk properties, while in a DMS calculation, trajectory calculations are carried out within a time-accurate flow simulation and the final state of each particle after a trajectory calculation becomes its initial state for the next trajectory. Consequently DMS can be used directly to simulate transient flows and can resolve non-Boltzmann conditions [3,34,35]. For the purpose of this section we will only consider trajectories involving N_2-N_2 interactions.

Similar to DSMC, the DMS method simulates only a fraction of real molecules in the volume of interest; enough to resolve the local distribution functions to a desired precision. A simulated molecule therefore represents a large number (W_p) of identical real molecules. Also, similar to DSMC, the DMS method moves simulated molecules without interaction for time steps on the order of the local mean-collision-time (τ_c) and also randomizes the impact parameters (and initial orientations) of colliding molecules by choosing collision pairs randomly within each small volume (typically a cube of dimension equal to one mean-free-path).

For the zero-dimensional relaxation calculations presented in this article, particle movement is not required and only a single flow volume is considered. Therefore a zero-dimensional DMS simulation advances with time steps on the order of τ_c and, at each time step, particle pairs are randomly selected within the volume for trajectories. The main difference compared to DSMC is that instead of using phenomenological probabilistic models to determine the collision rate and collision outcomes, trajectories on a specified PES are performed instead. In this manner, the outcomes of the trajectories completely determine the post-collision states of the molecules in the system. These states then become the initial states for subsequent collisions during a future time step. This results in a direct simulation of an evolving gas system including translational-rotational-vibrational energy exchange and dissociation and also allowing non-Boltzmann energy distributions to develop. The only model input to a DMS calculation is the PES and the simulation only operates on the positions and velocities of

atoms (whether bonded within a molecule or not). As a result, the DMS method makes no a-priori assumptions about decoupling of rotational and vibrational energy, rather rotational and vibrational energies of molecules are only calculated as a post-processing step in order to analyze the simulations for model development.

The core DMS algorithm is relatively straight-forward and has been described in detail in prior publications [3,36], however, we briefly summarize the method here for clarity. Given an initialized system of N_p molecules with weight W_p in a volume V (initialization is discussed later), during each DMS time step (Δt_{DMS}), a conservative number ($N_{T\text{-}max}$) of molecules pairs are randomly selected for trajectories, based on a maximum expected collision rate:

$$N_{t\text{-}max} = \frac{1}{2} N_p \left(N_p - 1\right) \frac{(\sigma g)_{max} W_p \Delta t_{DMS}}{V}. \qquad (1)$$

Here, σ is an appropriate collision cross-section (discussed later) and g is the center-of-mass relative velocity of the molecule pair. The value $(\sigma g)_{max}$ is a conservative estimate for the maximum value found for all collision pairs and can be updated during the simulation.

The value of $N_{T\text{-}max}$ is rounded to the nearest integer ($N^*_{T\text{-}max}$) and this number of molecule pairs are randomly selected within the volume. Next, each of the $N^*_{T\text{-}max}$ pairs are accepted for a trajectory calculation with probability P_T, given by

$$P_T = \frac{\sigma g}{(\sigma g)_{max}} \left(\frac{N_{T\,max}}{N^*_{T\,max}} \right). \qquad (2)$$

Equations 1 and 2 form the standard No-Time-Counter collision rate model used in DSMC. When used in the DMS and DSMC methods, these equations result in the following average number of collisions per volume per time step:

$$N_T = < P_T > \times N^*_{T\,max} = \frac{1}{2} N_p \left(N_p - 1\right) \frac{< \sigma g > W_p \Delta t_{DMS}}{V}. \qquad (3)$$

This is precisely the expression for the collision rate of the gas, where $<P_t>$ and $<\sigma g>$ represent the average taken over the molecule pairs. Note that the conservative estimate $(\sigma g)_{max}$ does not affect the collision rate.

Once the molecules pairs are selected for trajectories (using Eqns. 1 and 2), a trajectory calculation is performed for each pair, similar to the QCT method. A detailed description of the initialization of these trajectories, involving two particles can be found in Refs [3,35]. The two body trajectories are carried out in a relative coordinate system. Specifically, for a trajectory involving two particles A and B as illustrated in Fig. 3:

1. Particle A is placed at the origin and particle B is placed at a distance D_{cutoff} from A on the x-axis. B is then displaced by an impact parameter $b = b_{max} \times R_{f1}^{1/2}$ and rotated by a random angle $\theta = 2\pi R_{f2}$ on the y-z plane. Here R_{f1}, R_{f2} denote random numbers between zero and one. The pair is given a relative velocity $|g|$, which is obtained from the center of mass velocities of the pair.
2. Particle B is rotated about the origin to align the relative velocity vector with $\bar{g}$.
3. The atom positions and velocities relative to the center of mass of each molecule are known from the system initialization or from the particle's previous trajectory

4. The trajectory is advanced using a Velocity-Verlet integrator technique, which integrates the equations of motion:

$$F = m\frac{d\vec{v}}{dt} = -\nabla_r V(r) \quad (4)$$

where

$$\frac{d\vec{r}}{dt} = \vec{v} \quad (5)$$

Here, r is the atomic position vector, v is the atomic velocity vector, m is the mass of the atom and V is the potential energy given by the PES. The trajectories are integrated until the minimum separation between atoms (not bonded within the same molecule) becomes greater than D_{cutoff}.

5. Atomic positions and velocities for both pre- and post-states are available for post-processing. Most importantly, each particle exiting a trajectory maintains its new atomic positions and velocities (relative to the center of mass) as the initial state for the particle's next trajectory.

Similar to QCT, trajectories are initialized with an impact parameter b, such that $0 < b < b_{max}$. As described in previous publications [3,36] the appropriate cross-section to use in Eqs. 1 and 2 is therefore a hard-sphere cross-section corresponding to b_{max}: $\sigma = \pi b^2_{max}$. The value of b_{max} should be chosen conservatively, but the particular value of b_{max} has no effect on the solution [35]. For example, a larger value of b_{max} will lead to the calculation of more trajectories (via Eq. 2). However, since the trajectories are initialized with $0 < b < b_{max}$, many trajectories would have large values of b which would result in no deflection or change in energies (i.e. no "collision"). A smaller value of b_{max} results in fewer trajectories, however each trajectory is more likely to result in a change in molecule properties. In this manner, as long as b_{max} is chosen conservatively so as to capture all relevant collision dynamics its precise value has no effect on the simulated collision rate or collision outcomes, both of which result entirely from the PES. This has been explained and demonstrated in Ref. 36. For the simulations discussed in this article, $b_{max} = 6$ Å and $D_{cutoff} = 15$ Å.

The DMS calculations presented in this article focus only on internal energy transfer and dissociation processes for N_2-N_2 collisions. If a trajectory results in the dissociation of a molecule, the resulting atoms are simply removed from the simulation. As a result, the density, and therefore, collision rate change during the simulation. As described below, this is accounted for when interpreting the results. DMS simulations including both N_2 molecules and N atoms have been studied in other articles [37].

Relaxation calculations were carried out using both, the Ames PES and the Minnesota PES and the history of the system composition and internal energy distributions were compared. Similar to previous studies [3,34] the translational temperature (T_{tr}) of the system was kept constant by resampling (i.e. resetting) the center-of-mass velocities of all molecules using a Maxwell-Boltzmann distribution after each DMS time step.

The system is initialized with atomic positions and velocities generated to correspond to nitrogen molecules drawn from Boltzmann energy distributions for the

given temperature (T). That is, at $t=0$, $T_{tr} = T_r = T_v = T$. During initialization only ($t=0$), molecule rotational and vibrational energies are sampled from quantized Boltzmann energy distributions corresponding to the specific PES used. The WKB method is used, following the algorithms outlined by Bender et al. [20] and discussed earlier. During DMS calculations, since only atomic positions and velocities are used, quantized internal energy states are not determined except for post-processing. As the system evolves, some of the molecules dissociate and, as a result, vibrational and rotational energy is removed from the system due to dissociation. This decrease in energy in vibrational and rotational modes shows up as a drop in vibrational and rotational temperatures. Here T_r and T_v are simply calculated as the average rotational and vibrational energies in the entire system, rescaled by the Boltzmann constant. Eventually, the vibrational and rotational temperatures level off at values lower than T_{tr}, a condition called the quasi-steady state (QSS). The QSS is characterized by time invariant, non-Boltzmann distributions for the vibrational and rotational energy modes. Once the system is in QSS, the dissociation rate coefficient is calculated from the rate of change of the N_2 density with time, by fitting the composition histories obtained by the DMS method to the rate law:

$$\frac{d[N_2]}{dt} = -k_D[N_2]^2, \qquad (6)$$

where k_D is the dissociation coefficient rate coefficient. It is important to note that these dissociation coefficients account for dissociation due to N_2 - N_2 collisions only.

An example for an isothermal relaxation can be seen in Fig 4. In this example the gas is initialized with $T_{tr} = T_r = T_v = 30{,}000K$ and the translational temperature is kept constant at $T_t = 30{,}000K$. As the system evolves, the vibrational and rotational temperatures drop before leveling off at $T_r \sim 23{,}4000K$ and $T_v \sim 20{,}800K$, after which the system is said to be in QSS. The density of the system was initialized as $\rho = 1.28$ kg/m^3. This can be set arbitrarily and leads to a specific time-scale for the collision rate and therefore system evolution.

Figure 5 shows the vibrational and rotational distribution functions of molecules in the QSS for the example discussed above. When compared with the equilibrium (Boltzmann) distribution at 30,000K it is observed that the QSS distributions have depleted populations at higher vibrational levels and rotational levels. This is due to the fact that molecules in higher levels are more frequently lost due to dissociation and the bound-bound collisional mechanisms that replenish the populations at these levels cannot keep up with the dissociation process. As a result, the population distribution in QSS is inherently non-Boltzmann. These results are presented for demonstrative purpose and are taken directly from earlier publications [3,34].

Results and Discussion

Figure 6 shows a comparison of the thermal rate coefficients for $N_2 + N \rightarrow N + N + N$. The QCT rate coefficients from NASA[4,5] and Esposito et al.[18] at Bari University are compared with the results of shock tube experiments carried out by Appleton et al.[38], Hanson and Baganoff [39], and the 2-temperature hypersonic chemistry model developed by Park[40-42] which is currently the de facto standard for

aerothermodynamic modeling. Appleton's shock-tube experiments were carried out for a temperature range of 8000K to 15,000K and have a published uncertainty of ± 37%. Hanson and Baganoff's measurements were carried out for temperatures between 5700K and 12,000K and the uncertainty estimate was not given. The experimental and 2-temperature model rate coefficients are shown as 3-parameter Arrhenius fits extrapolated to the full temperature range in this figure. The concave curvature in the Hanson curve is for temperatures well above the range of their measurements and should not be considered physically meaningful. The NASA rate coefficients were computed for $7500 < T < 25{,}000K$. The Bari data[18] were computed for $1000 < T < 10{,}000K$ using the LEPS potential of Laganà et al.[17]. The overall agreement between Ames, Appleton and Park is quite good. The Bari data are in reasonably good agreement with the other data sets for $T < 10{,}000K$, but extrapolation of their results to higher temperature leads to large differences from the other rate coefficient data. Using the NASA PES, QSS rate coefficients have been determined from ME calculation[2]. The thermal and QSS rate coefficients are compared in Table 1. The QSS values are smaller than the thermal values by a factor of 0.65 to 0.5, with the larger difference at higher temperature. This is a consequence of preferential dissociation from high-lying ro-vibrational levels whose populations are depleted as the ensemble of N_2 molecules relaxes.

Table 1. Rate Coefficients for $N_2 + N \rightarrow N + N + N$ from QCT and ME Calculations

Temperature (K)	$k_D^{thermal}$ NASA ($cm^3molec^{-1}s^{-1}$)	k_D^{QSS} NASA ($cm^3molec^{-1}s^{-1}$)
7,500	3.320×10^{-15}	2.180×10^{-15}
10,000	1.310×10^{-13}	8.140×10^{-14}
12,500	1.081×10^{-12}	
15,000	4.337×10^{-12}	
20,000	2.280×10^{-11}	1.260×10^{-11}
25,000	5.878×10^{-11}	
30,000	1.010×10^{-10}	5.390×10^{-11}

Figure 7 shows a comparison of thermal rate coefficients for $N_2 + N_2 \rightarrow N + N + N_2$. The NASA[8] and Minnesota[19,20] values are compared with Appleton[38], Hanson and Baganoff [39], Thielen and Roth[44] and the Park 2-T model[40-42]. The comments made concerning the Appleton and Hanson results for $N_2 + N$ apply here as well. The Thielen and Roth measurements were made for a temperature range of 3390 K to 6435 K and no experimental uncertainty was given. That study was primarily concerned with measuring dissociation rate coefficients for $N_2 + Ar$ collisions and introduced a multiplicative factor $\beta_{N2} = k(N_2+N)/k(N_2+Ar)$ with the assumption that this ratio is independent of temperature. The best Arrhenius fit to the experiments with a range of initial N_2 mole fractions yielded a value of 2.5 for β_{N2}. The NASA[8] and

[8] The thermal rate coefficients given in Ref. 4 are incorrect as a result of an inadvertent computer error. The corrected values are given in Table 2.

Minnesota thermal rate coefficients are also summarized in Table 2 along with the QSS rate coefficients described below. The overall agreement between these data for the NASA and Minnesota PESs is excellent, but these rate coefficients are 2-4 times larger than the data from Appleton et al.[38] over the temperature range of that shock tube experiment (from 8000K to 15,000K).

We have carried out DMS calculations to compare isothermal relaxations using both the NASA and Minnesota PESs for T_t=10,000K, 15,000K, 20,000K and 30,000K. For the T_t=30,000K and 20,000K simulations 1×10^6 DMS molecules (N_p) were used, and for the T_t=10,000K and 15,000K cases 60,000 DMS molecules were used. The particle weight (W_p) for all simulations was set to one. The density for all simulations was set to 1.28 kg/m^3.The calculations for N_2-N_2 using the Minnesota PES developed by Paukku et al.[9] were reported previously by Valentini et. al [3]. New DMS calculations for N_2 - N_2 using the NASA PES developed by Jaffe et al.[8] at NASA Ames Research Center are carried out for the present study. The DMS method (and simulation code) used is identical to that used in Ref. 3 where the subroutine for the NASA Ames PES is called instead of the one for the Minnesota PES.

Table 2. Rate Coefficients for $N_2 + N_2 \rightarrow N_2 + N + N$ from QCT and DMS Calculations

Temperature (K)	$k_D^{thermal}$ NASA ($cm^3molec^{-1}s^{-1}$)	$k_D^{thermal}$ Minn. ($cm^3molec^{-1}s^{-1}$)	k_D^{QSS} NASA ($cm^3molec^{-1}s^{-1}$)	k_D^{QSS} Minn. ($cm^3molec^{-1}s^{-1}$)
8,000	4.38×10^{-15}	4.60×10^{-15}		
10,000	6.64×10^{-14}	7.10×10^{-14}	4.67×10^{-14}	1.98×10^{-14}
13,000	9.43×10^{-13}	9.13×10^{-13}		
15,000	2.74×10^{-12}		8.78×10^{-13}	7.99×10^{-13}
20,000	1.76×10^{-11}	1.63×10^{-11}	3.92×10^{-12}	3.30×10^{-12}
30,000	1.09×10^{-10}	8.51×10^{-11}	1.88×10^{-11}	1.81×10^{-11}

Figure 8(a)-(c) shows the composition histories for isothermal relaxations at T_t = 30,000K, 20,000K, 15,000K and 10,000K, respectively. Comparing the number of N_2 molecules remaining in the system versus time, it is clear that the rate of dissociation increases with increased T_t as expected. The composition histories, and therefore the rates of dissociation predicted by both PESs, are in remarkable agreement for T_t = 30,000K and 20,000K cases. A noticeable difference is seen for the T_t = 10,000K case where using the NASA PES predicts a higher dissociation rate than does using the Minnesota PES. However, for this case, the relaxation is in its early stages as less than 10% of the initial N_2 molecules have dissociated. To quantify the rate of dissociation at each temperature, dissociation rate coefficients are calculated using Eq. 6. After an initial period of simulation time, the slope of the N_2 density (e.g., in Fig. 8) decreases at a near constant rate. This is the QSS condition. The QSS rate coefficients for N_2 dissociation obtained for the interactions modeled by the NASA PES and Minnesota PESs are be given in Table 1 along with the thermal rate coefficients discussed earlier. It is apparent from the table and Fig. 8 that the thermal and QSS dissociation rate

coefficients predicted by the two potentials agree very well. Furthermore, these dissociation rate coefficients are compared with Arrhenius fit of the dissociation rate coefficients inferred from shock-tube experiments performed by Appleton et. al.[38] in Fig 9. It should be noted that the Appleton experimental data were measured at temperatures between 8,000K and 15,000K, so the values at 20,000K and 30,000K are extrapolations. It is apparent from the figure that there is good agreement between the rate coefficients obtained from the DMS calculations and the experimental values. Additional experimental data from Hanson and Baganoff[39] and Thielen and Roth[44] are also shown in Fig. 9. The predictions of both the NASA Ames and Minnesota PESs lie within the experimental uncertainty and, compared to the variation in measured rates, the agreement between the PESs is remarkably close, even at 10,000K. The thermal rate coefficients given in Table 2 for the Minnesota PES are 4 -5 times larger than the QSS values. For the NASA PES, the 20,000K and 30,000K values show a similar ratio between thermal and QSS, but the thermal:QSS ratio for 10,000K is only 1.4. This may signify a difference between the NASA and Minnesota PESs, or it may signify that the QSS condition has not been established for 10,000K DMS solution. QSS rate coefficients are usually smaller than thermal ones at high temperatures, because high ro-vibrational levels, which are more reactive, tend to get depleted during relaxation to thermochemical equilibrium.

Next, we analyze the vibrational and rotational distribution functions of molecules in QSS, as well as the pre-collision distributions of molecules that dissociate. These distributions are shown for all three cases in Fig. 10. It should be noted that the two PESs [8,9] were developed independently and have several differences. The difference that is relevant for this discussion is that the Ames PES supports 61 N_2 vibrational levels and 279 rotational levels while the Minnesota PES supports 55 vibrational levels and 279 rotational levels.

Vibrational distribution functions for the molecules in QSS are given by the dashed curves labeled as "system in QSS" in Fig 10 (a, c and e). For all three cases, the vibrational distribution functions for the system in QSS are non-Boltzmann due to a depletion of higher v levels due to preferential dissociation. For the T_t = 30,000K and 20,000K cases (Fig 10 (a and c) the distributions for the system in QSS coincide up to $v \sim 47$ $(f(v) \sim O(10^{-5}))$ beyond which the distributions diverge. The divergence of the distribution functions in the tail is due to the two PESs having different number of levels. Therefore, for the bulk of the molecules in QSS, the two PESs predict almost the same vibrational level populations. For the T_t = 10,000K case the system distributions do not precisely coincide but are very similar. The NASA PES result has a greater population than the Minnesota PES for levels $v > 10$. This larger population of higher vibrational levels is consistent with the higher dissociation rate predicted by the Ames PES (a factor of 2.36 times higher than the Minnesota PES, as noted earlier). However, it is also possible that the T_t = 10,000K case has not reached the QSS condition.

The vibrational distributions of the pre-collision states of dissociating molecules are shown as solid curves in Fig 10 (a, c, and e). As seen in prior publications [3,34], the pre-collision distributions for the dissociating species become flatter as T_t increases. At T_t = 10,000K (Fig 10 (e)) most dissociation is from the higher v levels. Since the

underlying populations of such high *v* levels are very small at that temperature, this reveals strong vibrational favoring in the dissociation process as documented in detail in Ref. 34. However at higher T_t (Fig 10 (a and c)), dissociation occurs from all levels due to the higher translational energies available in the collisions. All distribution functions in the QSS predicted by both the NASA and Minnesota PESs agree remarkably well. Upon close inspection, we see that the NASA PES has less dissociation from lower *v* levels and overshoots the distribution obtained by the Minnesota PES in the middle before dropping down at the distribution obtained by the Minnesota PES at the tail end of the distribution.

The rotational distribution functions of molecules in QSS are given by the dashed curves labeled as "system in QSS" in Fig 10 (b, d and f). For all the three cases the rotational distribution functions are non-Boltzmann due to depletion of high *J* levels. The rotational distribution of the pre-collision states of dissociating molecules is given by the solid curves in Fig 10 (b, d and f). In all three cases the rotational distribution of the pre-collision states of dissociating molecules are non-Boltzmann, as observed in previous work [34]. For all cases, the distributions obtained from the two PESs agree almost exactly, except at the tail of the distribution. As pointed out earlier, the difference at the tail of the distribution is due to the difference in the number of the ro-vibrational levels in the two PESs.

The calculations of the potential energy surfaces and rate coefficients do not contain empirical parameters that can be adjusted to reproduce specific experimental data. The fact that there is generally good agreement between the experimental dissociation rate coefficients[38,39,43] and the computed QCT rate coefficients provides validation of the physics-based computational approach.

Conclusions

In this paper we have attempted to evaluate the accuracy of potential energy surfaces based on quantum mechanical calculations and of rate coefficients computed using classical mechanics based on these potentials. In the last ten years a number of such PESs have been prepared to describe atom-diatom and diatom-diatom collisions. Since the mid-1990s, most of these potentials have been based on the same group of methods for solving the electronic Schrodinger equation – CCSD(T), CASSCF-MRCI and CASPT2 using correlation consistent-polarized valence atomic orbital basis sets. For the 3-atom systems, the resulting rate coefficients computed using these potentials are in good agreement with the generally accepted experimental data for high-temperature exchange and dissociation reactions encountered in modeling combustion chemistry and hypersonic atmospheric entries of spacecraft. It must be noted that there is no calibration required or attempted with these rate coefficients.

We have used the collisional dissociation of N_2 to assess the current state-of-the-art of theoretical and computational methods for determining these rate coefficients. We use N_2 + N to illustrated this approach for atom-diatom cases. The rate coefficients determined using the NASA PES for N_3 are in excellent agreement with shock tube experiments, and superior to calculations using empirical and semi-empirical potentials.

For 4-atom systems, the best test case is dissociation of N_2 due to $N_2 + N_2$ collisions because there are two independent PESs in the recent literature. We have compared thermal rate coefficients computed by the QCT method using the different potentials from NASA Ames and the University of Minnesota and found them to be nearly identical for temperatures above 10,000K. We have also computed rate coefficients under QSS conditions using the DMS method and found similar results. The QSS rate coefficients are also in very good agreement with the results of shock tube experiments. Therefore, we believe rate coefficients computed in this fashion can be used with confidence in Computational Fluid Dynamics (CFD) modeling for aerothermodynamics applications.

References

1. R. L. Jaffe, D. W. Schwenke and M. Panesi, "First Principles Calculation of Heavy Particle Rate Coefficients", in "Hypersonic Nonequilibrium Flows: Fundamentals and Recent Advances", E. Josyula, ed., Progress in Astronautics and Aeronautics, Vol. 247, (AIAA, Reston, VA, 2015), pp 103-158.

2. M. Panesi, R. L. Jaffe, D. W. Schwenke, and T. E. Magin, "Rovibrational internal energy transfer and dissociation of $N_2(^1\Sigma_g^+)$-$N(^4S_u)$ system in hypersonic flows", J. Chem. Phys. **138**, 044312 (2013).

3. P. Valenti, T. E. Schwartzentruber, J. D. Bender, I. Nompelis and G. V. Candler, "Direct Simulation of rovibrational excitation and dissociation in molecular nitrogen using an ab initio potential energy surface", AIAA Sci-Tech Conference, Kissimmee, FL, January 2015 AIAA-2015-0474.

4. R. L. Jaffe, D. W. Schwenke, G. Chaban and W. M. Huo, "Vibrational and Rotational Excitation and Relaxation of Nitrogen from Accurate Theoretical Calculations," AIAA 2008-1208, presented at the 46th AIAA Aerospace Sciences Meeting and Exhibit, January 2008, Reno, Nevada.

5. R. L. Jaffe, D. W. Schwenke, G. Chaban, "Theoretical analysis of N_2 collisional dissociation and rotation-vibration energy transfer", 47th AIAA Aerospace Sciences Meeting, Orlando, Florida, January 2009, AIAA 2009-1569.

6. E. Garcia, A. Saracibar, S. Gómez-Carrasco and A. Laganà, "Modeling the Global Potential Energy Surface of the $N + N_2$ reaction from ab initio data", Phys. Chem. Chem. Phys. **10,** 2552-2558 (2008).

7. B. R. L. Galvao and A. J. C. Varandas, "Accurate Double Many-Body Expansion Potential Energy Surface for N_3 (^{4}A") from Correlation Scaled ab Initio Energies with Extrapolation to the Complete Basis Set Limit", J. Phys. Chem. A **113**, 14424-14430, (2009).

8. R. L. Jaffe, D. W. Schwenke, G. Chaban, "Vibrational and Rotational Excitation and Dissociation in N_2-N_2 Collisions from Accurate Theoretical Calculations", AIAA Thermophysics and Heat Transfer Conference, 28 June-1 July 2010, Chicago, IL, AIAA 2010-4517.

9. Y. Paukku, K. R. Yang, Z. Varga, and D. G. Truhlar, "Global ab initio ground-state potential energy surface of N_4", J. Chem. Phys. **139**, 044309 (2013); erratum ibid., **140**, 019903 (2014).

10. L. Pacifici, M. Verdicchio, N. F. Lago, A. Lombardi and A. Costantini, "A High-Level Ab Initio Study of the $N_2 + N_2$ Reaction Channel", J. Comp. Chem. **34**, 266802676 (2013).

11. H. Eyring and M. Polanyi, Z. Phys. Chem. B. **12**, 279 (1931).

12. F. London, Z. Electrochem. **35**, 552, (1929).

13. S. Sato, "On a New Method of Drawing the Potential Energy Surface", J. Chem. Phys. **23**, 592 (1955).

14. S. Sato, "Potential Energy Surface of the System of Three Atoms", J. Chem. Phys. **23**, 2465 (1955).

15. H. Eyring, "The Activated Complex in Chemical Reactions",J. Chem. Phys. **3**, 107-115 (1935).

16. M. Karplus, R. N. Porter and R. D. Sharma, "Exchange reactions with activation energy. I. Simple barrier potential for (H, H_2)", J. Chem. Phys. **43**, 3259-3287 (1965).

17. A. Laganà, E. Garcia, and L. Ciccarelli, "Deactivation of Vibrationally Excited Nitrogen Molecules by Collision with Nitrogen Atoms", J. Phys. Chem. **91**, 312-314 (1987).

18. F. Esposito, I. Armenise, and M. Capitelli, "N-N_2 state to state vibrational-relaxation and dissociation rates based on quasiclassical calculations", Chem. Phys., **331** (1), 1–8 (2006).

19. J. D. Bender, I. Nompelis, P. Valentini, S. Doraiswamy, T. Schwartzentruber, and G. V. Candler, "Quasiclassical Trajectory Analysis of $N_2 + N_2$ Reaction Using a New Ab Initio Potential Energy Surface", 11th AIAA/ASME Joint thermophysics and heat Transfer Conference, Atlanta, GA, June 2014 AIAA-2014-2964.

20. J. D. Bender, P. Valentini, I. Nompelis, Y. Paukku, Z. Varga, D. G. Truhlar,T. Schwartzentruber, and G. V. Candler, "An Improved Initio Potential Energy Surface and Multi-Temperature Trajectory Calculations of $N_2 + N_2$ Dissociation Reactions",J. Chem. Phys. **143**, 054304 (2015).

21. T. H. Dunning, J. Chem. Phys. **90**, 1007-1023 (1989).

22. R. A. Kendall, T. H. Dunnng and R. J. Harrison, J. Chem. Phys. **96**, 6796 (1992).

23. G. D. Purvis and R. J. Bartlett, "A Full Coupled-cluster Singles and Doubles Model: The Inclusion of Disconnected Triples", J. Chem. Phys. **76** (2), 1910-1918 (1982).

24. R.J. Gdanitz and R. Ahlrichs, "The averaged coupled-pair functional (ACPF): A size-extensive modification of MR CI(SD)", Chem. Phys. Lett. **143** (4), 413-420 (1988).

25. B.O. Roos, P.R. Taylor and P.E.M. Siegbahn, "A Complete Active Space SCF Method (CASSCF) Using a Density Matrix Formulated Super-CI Approach", Chem. Phys. **48** (2), 157-173 (1980).

26. R.J. LeRoy, Y. Huang and C. Jary, "An accurate analytic potential function for ground-state N_2 from a direct-potential-fit analysis of spectroscopic data", J. Chem. Phys. **125**, 164310 (2006).

27. L. I. Schiff, "Quantum Mechanics", Third Ed. (McGraw-Hill, New York, 1955), 268-279.

28. P. J. Knowles and H. –J. Werner, Chem. Phys. Lett. **115**, 259 (1985).

29. D. W. Schwenke and M. Panesi, unpublished.

30. G. A. Bird, "Molecular Gas Dynamics and Direct Simulation of Gas Flows", Clarendon, Oxford, 1994.

31. K. Koura, "Monte Carlo direct simulation of rotational relaxation of diatomic molecules using classical trajectory calculations: nitrogen shock wave," Phys. Fluids **9** (11), 3543–3549 (1997).

32. K. Koura, "Monte Carlo direct simulation of rotational relaxation of nitrogen through high total temperature shock waves using classical trajectory calculations," Phys. Fluids **10** (10), 2689–2691 (1998).

33. H. Matsumoto and K. Koura, "Comparison of velocity distribution functions in argon shock wave between experiments and Monte Carlo calculations for Lennard-Jones potential," Phys. Fluids **3** (12), 3038–3045 (1991).

34. P. Valentini and T. E. Schwartzentruber,"Direct molecular simulation of high-temperature nitrogen dissociation due to both N-N_2 and N_2-N_2 collisions", AIAA Aviation 22-26 June 2015, Dallas,TX, AIAA-2015-3254.

35. M. S. Grover, P. Valentini and T. E. Schwartzentruber, “Coupled rotational-vibrational excitation in shock waves using trajectory-based direct simulation Monte Carlo”, AIAA SciTech, Kissimmee, FL, Jan. 2015, AIAA-2015-1656.

36. P. Norman, P. Valentini and T. Schwartzentruber, "GPU-accelerated Classical Trajectory Calculation Direct Simulation Monte Carlo applied to shock waves", J. Comp. Phys. **247**, 153-167 (2013).

37. P. Valentini and T. E. Schwartzentruber "Ab initio based model for high temperature nitrogen rovibrational excitation and dissociation", AIAA Sci-Tech Conference, San Diego, CA, January 2016, AIAA-2016-xxxx.

38. J. P. Appleton, M. Steinberg and D. J. Liquornik, “Shock-Tube Study of Nitrogen Dissociation using Vacuum-Ultraviolet Light Absorption”, J. Chem. Phys. **48** (2), 599-608 (1968).

39. R. K. Hanson and D. Baganoff, "Shock-Tube Study of Nitrogen Dissociation Rates Using Pressure Measurements" AIAA J. **10**, 211 (1972).

40. C. Park, "Assessment of Two-Temperature Kinetic Model for Dissociating Weakly-Ionizing Nitrogen," J. Thermophysics and Heat Transfer **2** (1), 8-16 (1988).

41. C. Park, J. T. Howe, R. L. Jaffe and G. V. Candler, Review of Chemical-Kinetic Problems of Future NASA Missions, II: Mars Entries”, J. Thermophysics and Heat Transfer **8** (1), 9-23 (1988).

42. C. Park, R. L. Jaffe and H. Partridge, “Chemical-Kinetic Parameters for Hyperbolic Earth Entry”, J. Thermophysics and Heat Transfer, **15** (1), 76-90 (2001).

43. K. Thielen and P. Roth, “N Atom Measurements in High-Temperature N_2 Dissociation Kinetics”, AIAA J. 24 (7), 1102-1105 (1986).

Figures

(a)

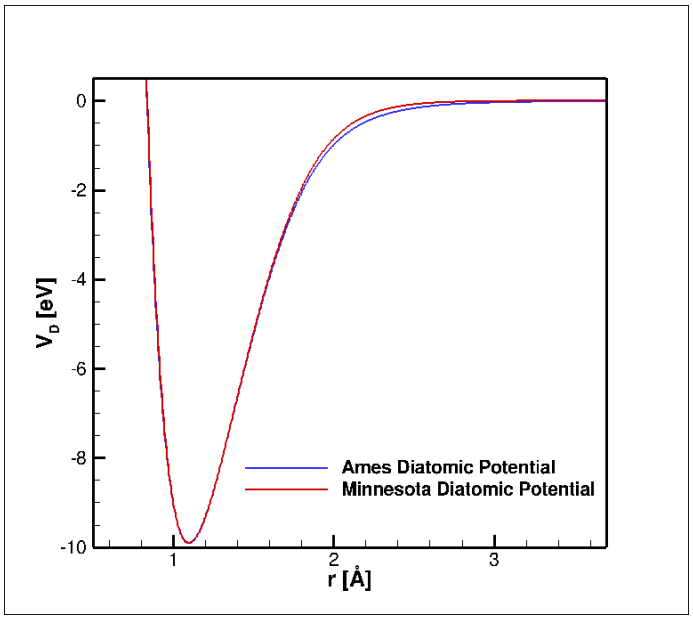

(b)

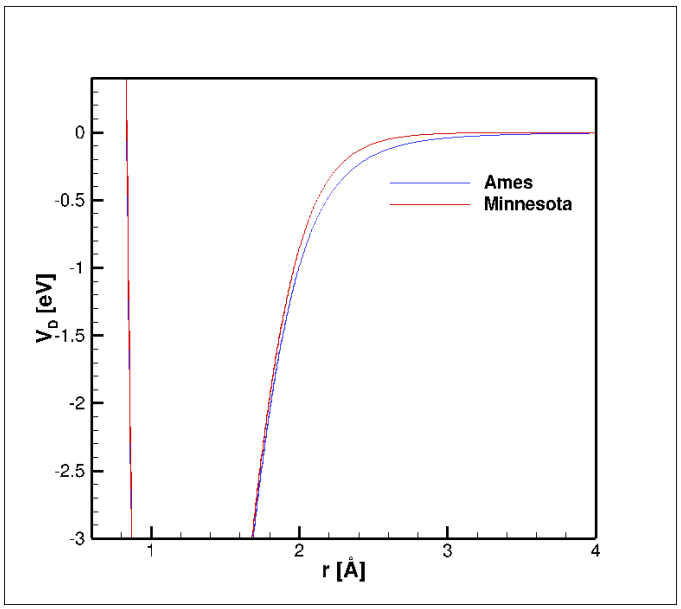

Figure 1. Comparison of the N_2 diatomic potentials used in the NASA and Minnesota PESs for $N_2 + N_2$ and $N_2 + N$. (a) shows the full potential curve and (b) shows the enlarged region for large r.

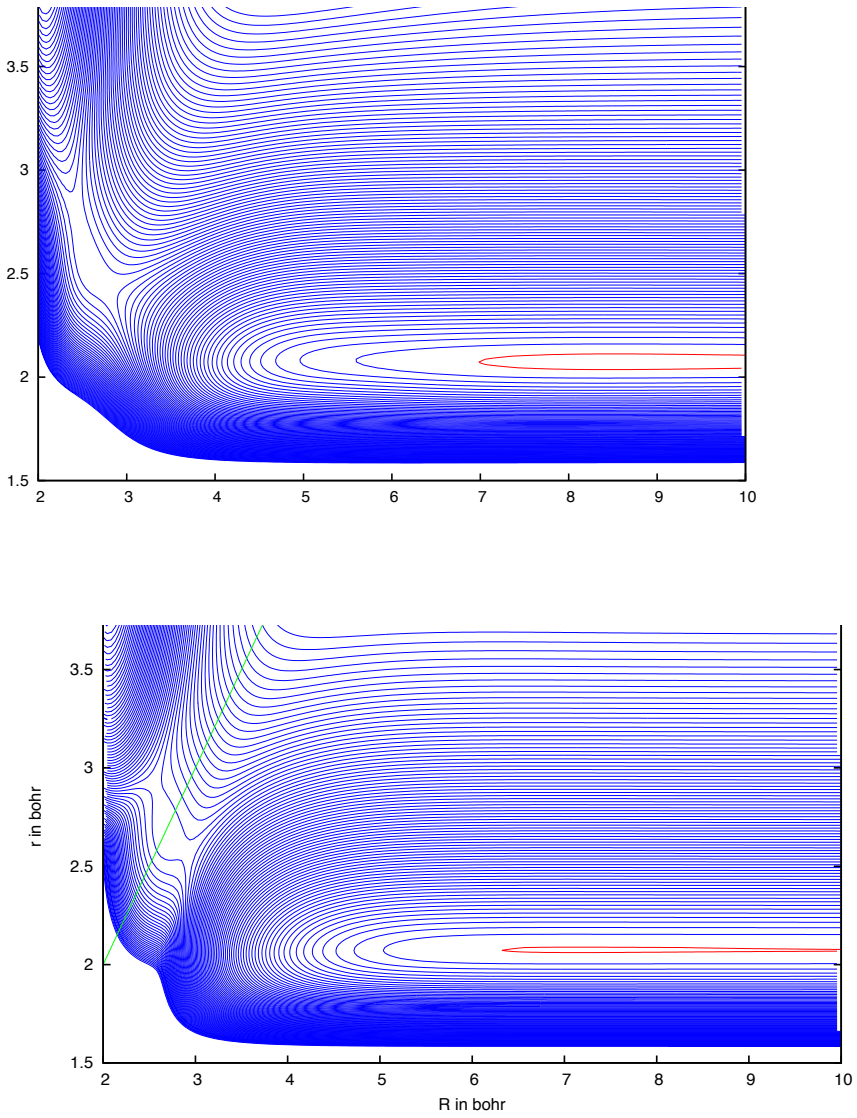

Figure 2. Comparison of the U. Minnesota[9] (top) and NASA[8] Ames (bottom) PESs for rectangular geometries of N_4. N atoms are at the corners of a rectangle. The potential energies are relative to two N_2 molecules with bond lengths at $r = r_e$ and $R = \infty$. Blue and red lines represent constant energy contours. The red contour has zero energy and each successive blue line represents a 5 kcal/mol increase in energy. The green line in the bottom plot represents the points where R = r.

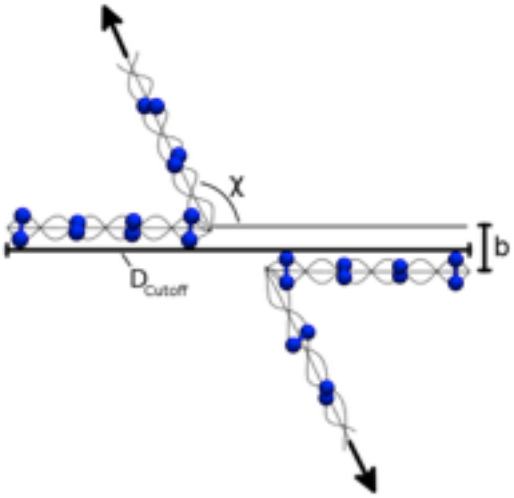

Figure 3. Set-up for a molecular trajectory in the DMS system.

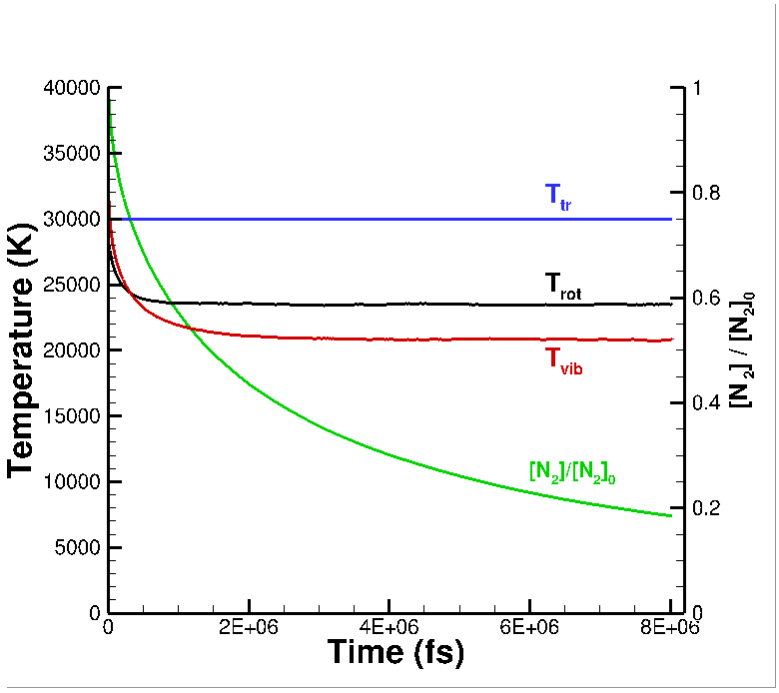

Figure 4. The temperature and composition history of an isothermal relaxation in a box at T = 30,000K. The blue curve represents the translational temperature, the black curve represents the rotational temperature and the red curve represents the vibrational temperature for the isothermal relaxation. The green curve represents the fraction of N_2 left in the system.

(a)

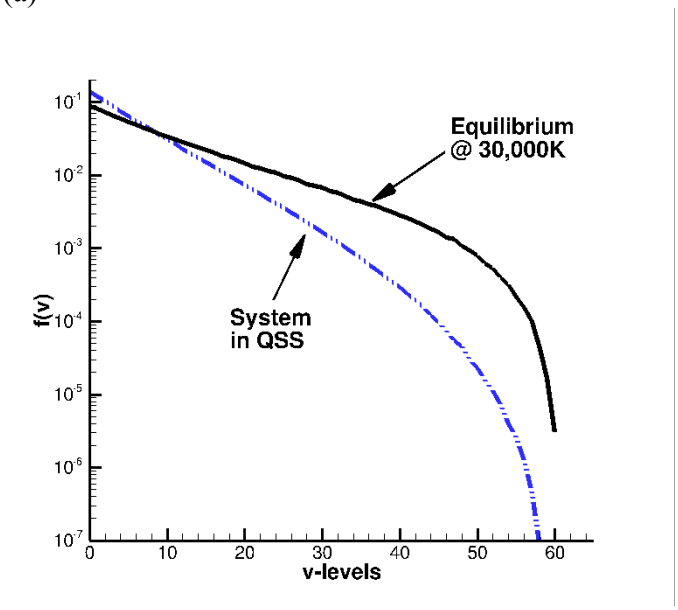

(b)

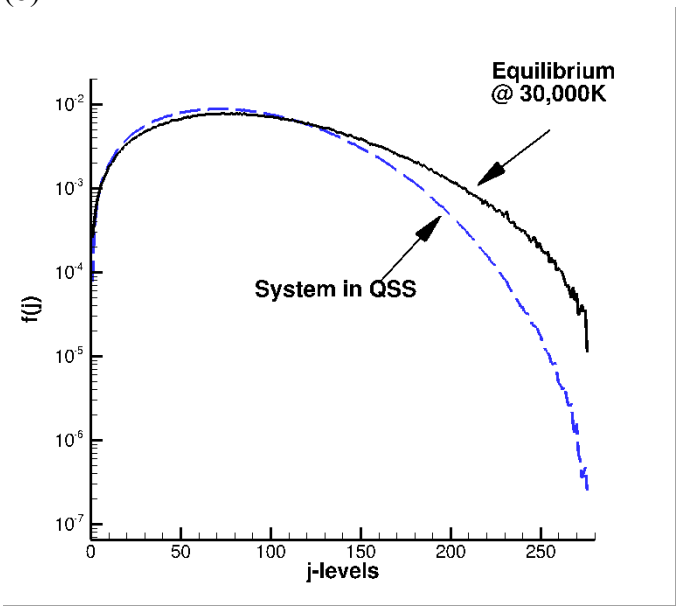

Figure 5. The vibrational (a) and rotational (b) distribution of N_2 molecules in QSS for T_t = 30,000K and the Boltzmann distribution at $T_v = T_r$ = 30,000K.

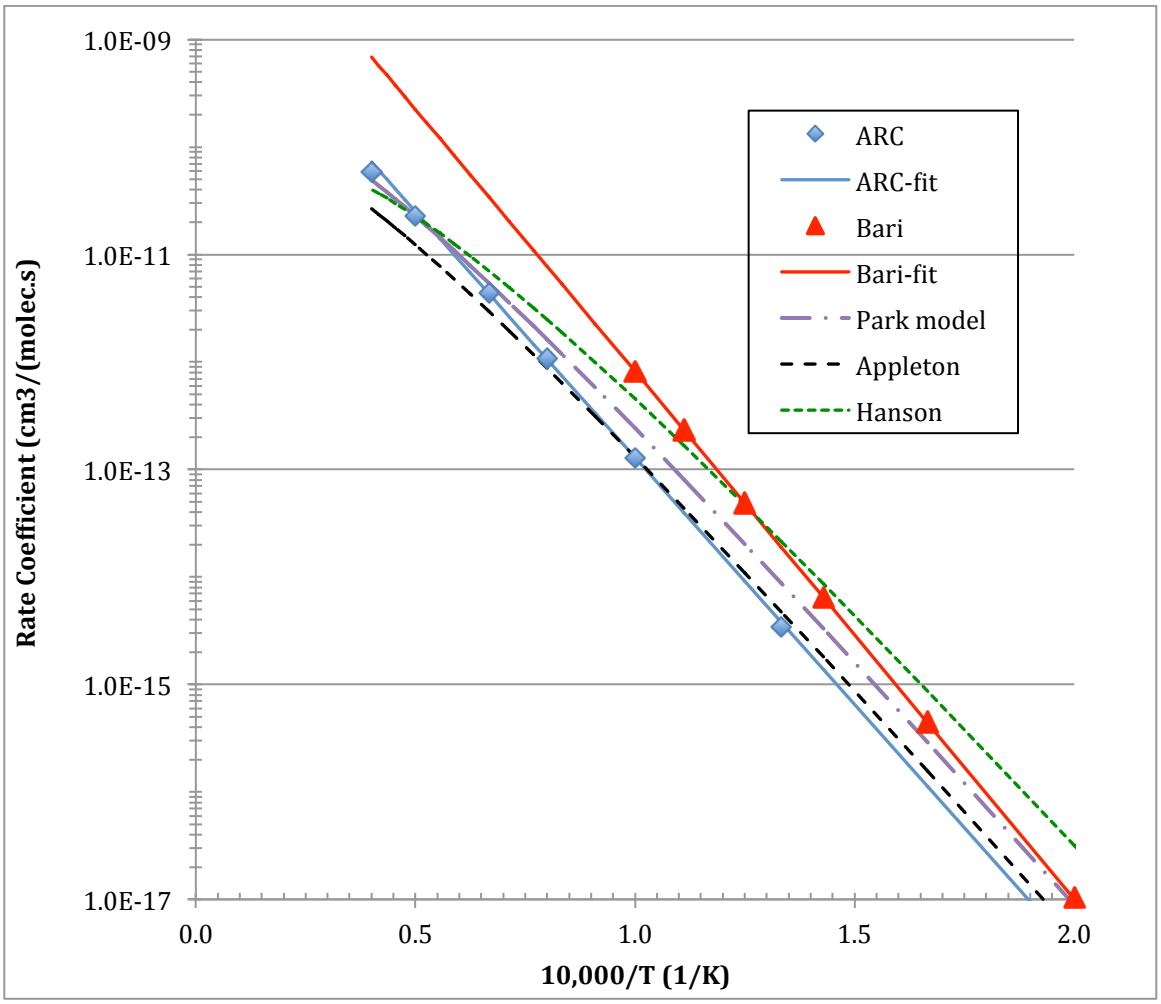

Figure 6. Thermal rate coefficients for $N_2 + N \rightarrow N + N + N$ between 5000K and 25,000K. Computed rate coefficients using the QCT method with the PES from NASA [4,5] and Esposito et al.[18] are compared. The symbols are the actual calculated values and the lines are for Arrhenius fits that have been extrapolated over the full temperature range. Also shown are extrapolated Arrhenius fits from shock-tube experiments by Appleton et al. [38] and Hanson and Baganoff[39] and from Park's 2-T model[40-42]. The Appleton experimental data was obtained for 8000K < T < 15,000K and the Hanson data was obtained for 5700K to 12,000K.

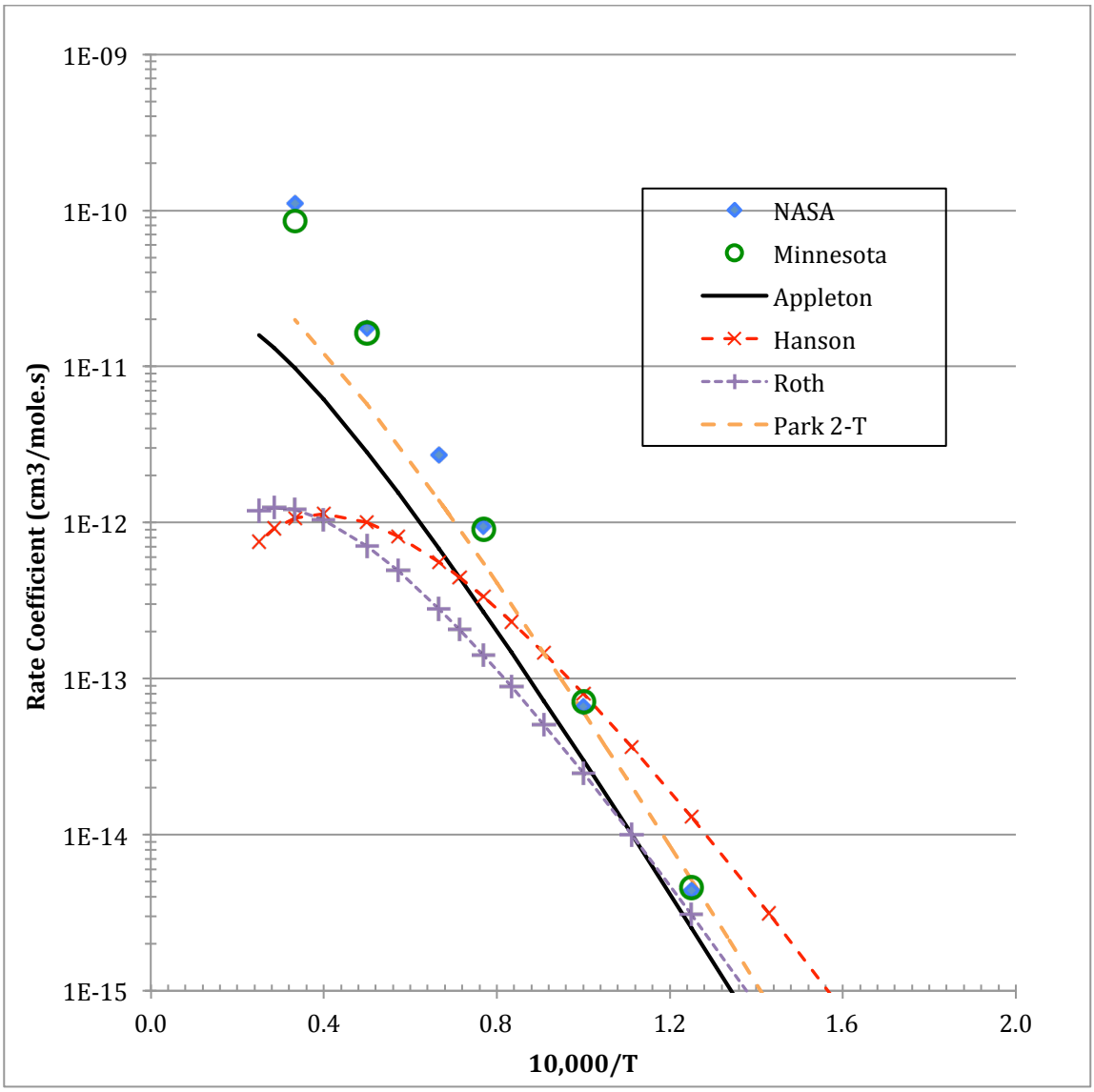

Figure 7. Thermal rate coefficients for $N_2 + N_2 \rightarrow N + N + N_2$. Computed rate coefficients using the QCT method using the NASA[8] (blue diamonds) and Minesota[9] (green circles) PESs are compared, along with values from shock-tube experiments of Appleton[38], Hanson[39], Roth[43] and Park's 2-T model[40,42].

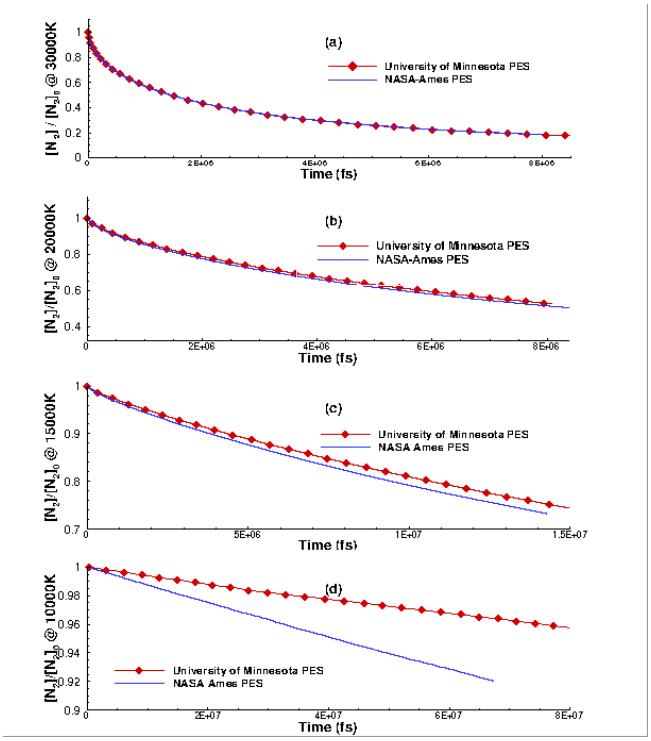

Figure 8. DMS composition histories for N_2+N_2 dissociation at (a)T_t = 30,000K, (b)T_t = 20,000K, (c) 15,000K and (d)T_t = 10,000K as the fraction of N_2 remaining in the system. The blue solid lines are the results obtained from the NASA PES while the red lines with symbols are the results obtained from the Minnesota PES.

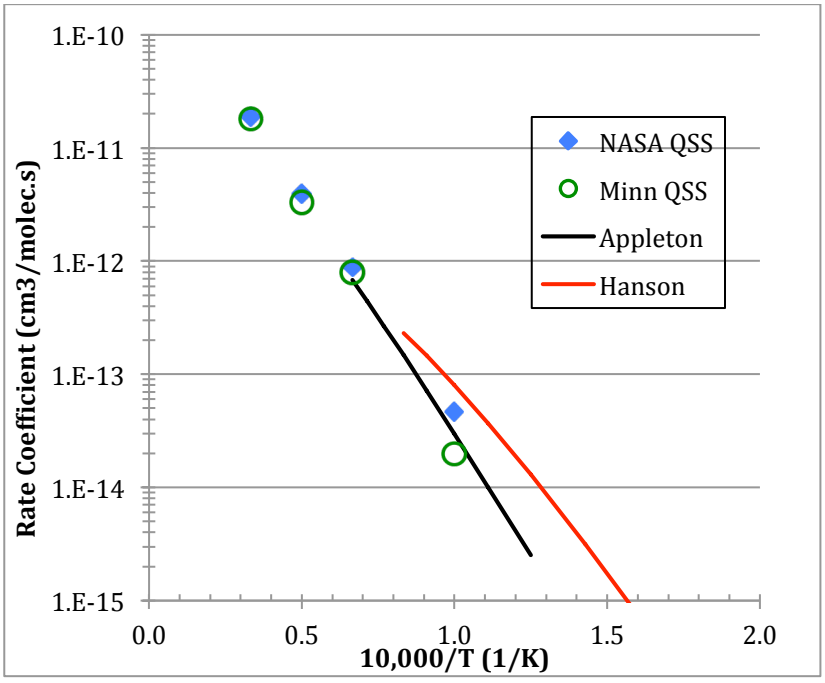

Figure 9. N_2+N_2 dissociation rate coefficients calculated for QSS conditions and compared with experimental data. See Fig. 7 for details.

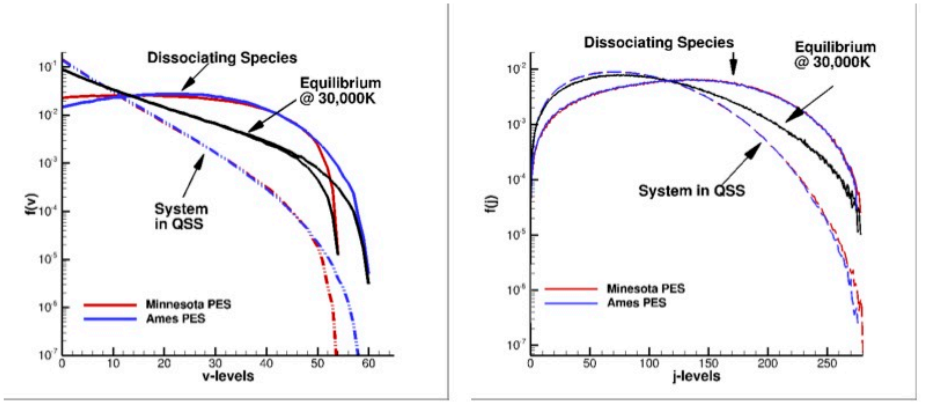

(a) Vibrational Energy Distributions at $T_t = 30000K$.

(b) Rotational Energy Distributions at $T_t = 30000K$

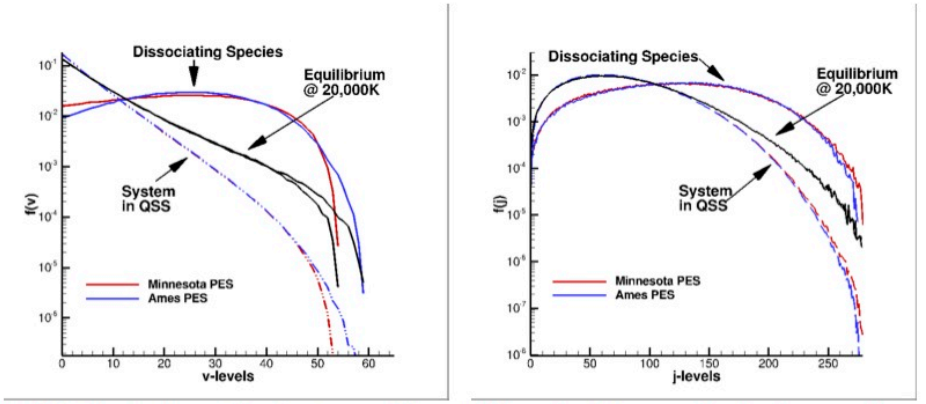

(c) Vibrational Energy Distributions at $T_t = 20000K$.

(d) Rotational Energy Distributions at $T_t = 20000K$

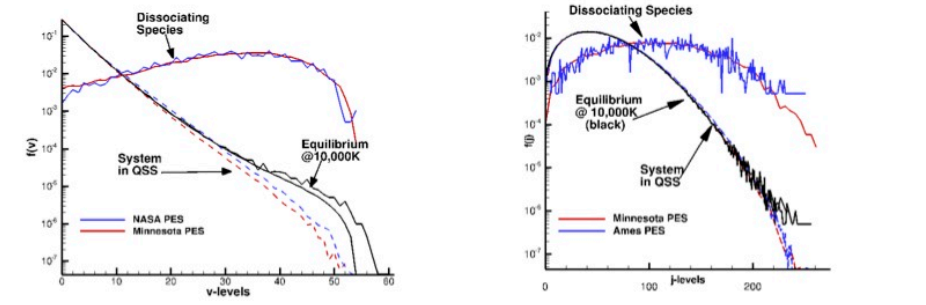

(e) Vibrational Energy Distributions at $T_t = 10000K$.

(f) Rotational Energy Distributions at $T_t = 10000K$

Figure 10. Vibrational and rotational distribution functions for the bound molecules in QSS and pre-collision states of dissociated molecules for the Ames (red) and Minnesota (blue) PESs for T_t = 30,000K, 20,000K and 10,000K from DMS calculation for N_2+N_2. The black curves are the equilibrium (Boltzmann) distribution at the corresponding temperatures. The solid lines labeled as "Dissociating Species" are distributions for the pre-collision states of dissociating molecules. The dashed lines labeled "System in QSS" are the distribution of the molecules in QSS.